

## Sensing Enhancement of Gold Nanoparticles Doped-TiO<sub>2</sub> Thin Films as H<sub>2</sub>S Gas Sensor

M.A. Alalousi<sup>1,a</sup>, Jamal M. Rzaij<sup>1,b\*</sup>, I.M. Ibrahim<sup>2,c</sup>, A. Ramizy<sup>1,d</sup>  
and M.H. Eisa<sup>3,e</sup>

<sup>1</sup>Department of Physics, College of Science University Of Anbar, Ramadi, Iraq

<sup>2</sup>Department of Physics, College of Science, University of Baghdad, Baghdad, Iraq

<sup>3</sup>Department of Physics, College of Science, Sudan University of Science and  
Technology, Khartoum 11113, Sudan

<sup>a</sup>mazin\_alalousi@uoanbar.edu.iq, <sup>b</sup>sc.jam72al@uoanar.edu.iq, <sup>c</sup>dr.issamiq@gmail.com,  
<sup>d</sup>asmat\_hadithi@uoanbar.edu.iq, <sup>e</sup>mheisas@hotmail.com

\*Corresponding author: Jamal M. Rzaij; E-mail: sc.jam72al@uoanbar.edu.iq

**Keywords:** TiO<sub>2</sub>, Au nanoparticle, Pulsed laser ablation, H<sub>2</sub>S, Spray pyrolysis, Gas sensor

**Abstract.** Titanium dioxide and gold nanoparticles were synthesized using an environmentally friendly method to deposit undoped and Au-doped TiO<sub>2</sub> thin films on silicon and glass substrates via the spray pyrolysis technique. The effect of the Au nanoparticles concentrations on structural, morphological, and hydrogen sulfide (H<sub>2</sub>S) gas sensing characteristics of TiO<sub>2</sub> thin films were investigated. An X-ray diffraction pattern confirmed the polycrystalline structure of the films deposited on glass and Si substrates with a dominant rutile phase and the formation of additional mixed-phases of Ti-Au bonding. According to a Field Emission-Scanning Electron Microscopy investigation, the cluster size ranged from 20 to 180 nm depending on the concentration of AuNPs. The sensing response of the prepared films was tested against H<sub>2</sub>S at different operating temperatures. The effect of growing a mixture of titanium-gold phases as a suitable catalyst for hydrogen sulfide sensitivity is also discussed.

### Introduction

Transition metal oxides, including TiO<sub>2</sub> electronic configuration, are reported as suitable gas sensors due to the properties of TiO<sub>2</sub>, such as abundance, affordability, and thermal stability [1]. TiO<sub>2</sub> gas sensor works in harsh, toxic, and high relative temperature environments. TiO<sub>2</sub> is extensively used in many applications, such as gas sensor devices, medical applications, decoration materials, and electronic devices [2]. TiO<sub>2</sub> exists in nature in four forms: rutile, anatase, brookite, and β-TiO<sub>2</sub> [3]. The rutile phase of grain size around 35 nm has better thermal stability than the anatase phase due to a shorter Ti-O bond length than the anatase phase [4]. The anatase phase is stable at 11-35 nm, while the brookite is stable at grain sizes less than 11 nm [5]. Semiconductor thin films of TiO<sub>2</sub> are intensively studied for gas sensing applications. However, TiO<sub>2</sub> does not respond actively as hydrogen sulfide (H<sub>2</sub>S) sensor at temperatures below 200 °C [6]. As a result, adding catalytic metals such as Au, Ag, Pt to TiO<sub>2</sub> is widespread [7],[8]. A strong Ti-Au bond prevents grain growth and slows down the anatase transformation, resulting in the restructuring of the surface by the interstitial Ti atoms and locally modifying the chemical reactivity [9]. The AuNPs play a significant role in enhancing TiO<sub>2</sub> sensing characteristics, and it reduces the operating temperature and increases the interaction between the sensor surface and the gas target [10].

Hydrogen sulfide is the most dangerous and toxic gas [11]. Therefore, TiO<sub>2</sub> gas sensor devices have been studied to demonstrate optimal operating conditions for detecting H<sub>2</sub>S.

In 2006 [12], Jakubik showed that temperature and wave frequency did not affect the sensitivity of TiO<sub>2</sub> thin films as a surface-acoustic-wave gas sensor. Also, in the same year, Chaudhari et al. confirmed that the sensitivity of Cu, Mo, and Al-doped TiO<sub>2</sub> was decreased at operating temperatures between (250-350) °C [11]. In 2010, Gaspera et al. reported an improvement in the sensitivity of Au

doped-TiO<sub>2</sub>-NiO films [13]. Furthermore, several investigations on the composition of TiO<sub>2</sub> for H<sub>2</sub>S sensing are studied; for example, E. Gazzola et al. [14] and L. FRANCIOSO et al. [15] demonstrated the synthesis of titanium dioxide doped/coated with gold nanoparticles thin films. However, they did not investigate the influence of structural phases formed between titanium and gold on TiO<sub>2</sub> gas sensing characteristics. As a result, it is possible to summarize the problem addressed by the current study as follows: There are few studies about the sensitivity of TiO<sub>2</sub> compounds to H<sub>2</sub>S because hydrogen sulfide gas has limited chemical activity at low temperatures. Furthermore, few researchers have investigated the effects of titanium-gold mixed-phase development as a suitable catalyst for the sensitivity of TiO<sub>2</sub> thin film to H<sub>2</sub>S gas.

In this study, undoped TiO<sub>2</sub> thin film and doped with Au nanoparticles were deposited on silicon and glass substrates using the chemical spray pyrolysis technique. The sensing response of the prepared films was tested against H<sub>2</sub>S at different operating temperatures. This study focuses on the effect of the growth of the titanium-gold mixed-phase as a suitable catalyst for hydrogen sulfide sensitivity.

## Experimental Procedure

### Materials and thin films synthesis

Pulsed laser ablation (Q-switched Nd: YAG laser type HUAFEI with wavelength 532 nm) was used to form TiO<sub>2</sub> and Au nanoparticles. A high-purity titanium dioxide nanoparticle powder (99.99% by NIST1898 Sigma-Aldrich) was used to form a pellet target with a diameter of 12 cm and thickness of 0.3 cm using a Hydraulic press under 10<sup>7</sup> N/m<sup>2</sup> for 60 minutes at room temperature. Pulsed laser ablation (PLA) was used to prepare the gold nano-colloidal solutions by using a high purity gold sheet (10×10×2) mm<sup>3</sup> as demonstrated earlier by Al-Alousi [16]. The TiO<sub>2</sub> pellet and gold sheet were separately mounted vertically on the laser beam within a cylindrical glass cell. Nano-colloidal solutions were synthesized in 15 ml deionized water. TiO<sub>2</sub> and Au nanoparticles (AuNPs) concentrations were determined to be 680 and 169 ppm, respectively, using an atomic absorption spectrometer (type GBC). The spray pyrolysis technique was used to deposit undoped and AuNPs-doped TiO<sub>2</sub> thin films (75±5 nm thick) of TiO<sub>2</sub> and TiO<sub>2</sub>: Au samples with different AuNPs colloidal solution volume ratios (1%, 3%, and 5%) deposited on glass and n-type (111) silicon substrates of low resistivity (0.004 Ω-cm) at 300 °C. The structural characteristics of the prepared films were investigated using an X-ray diffractometer (type Philips PW 1730) pattern with a diffraction angle (2θ) of 20° to 80°. The morphological feature of the samples was analyzed using a field emission-scanning electron microscope (Nova Nanosem 230) at magnifications of 5 and 20 Kx.

### Experimental setup

The gas sensing characteristics were investigated under dynamic flow conditions in a cylindrical stainless-steel chamber. The sensing response of TiO<sub>2</sub> and TiO<sub>2</sub>: Au thin films when exposed to 30 ppm H<sub>2</sub>S were measured in atmospheric air conditions at operating temperatures of 25, 50, 100, 150, and 200 °C. The gas sensor system is depicted in diagrammatic form in Fig. 1. The tested gas concentration was calculated by using the following equation: [17]

$$\text{gas concentration}_{ppm} = \text{gas parent concentration}_{(ppm)} \frac{\text{Flow rate of gas parent}}{\text{Total flow rate}} \quad (1)$$

where the total flow rate is the sum of both air and target gas flow rates.

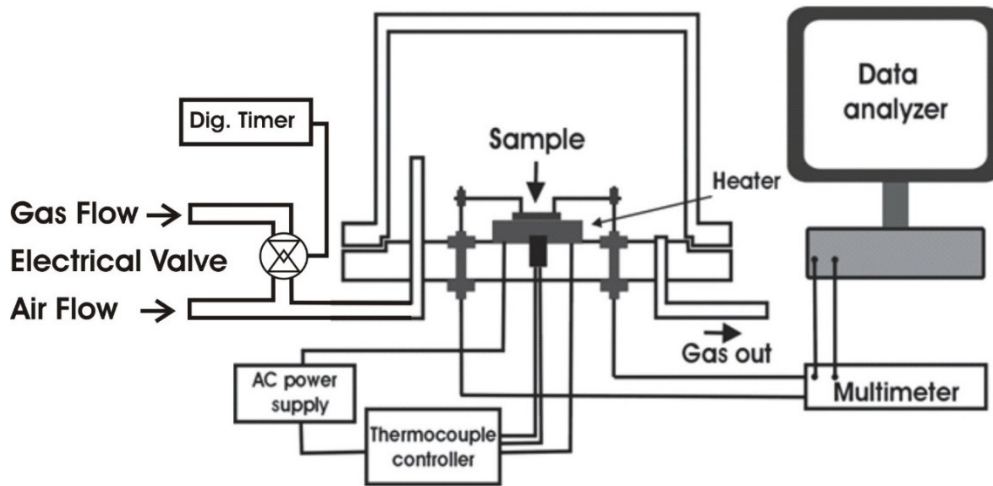


**Fig. 1: The schematic of the sensing test system.**

The sensitivity of the produced films when exposed to hydrogen sulfide was estimated based on the following equation: [18]

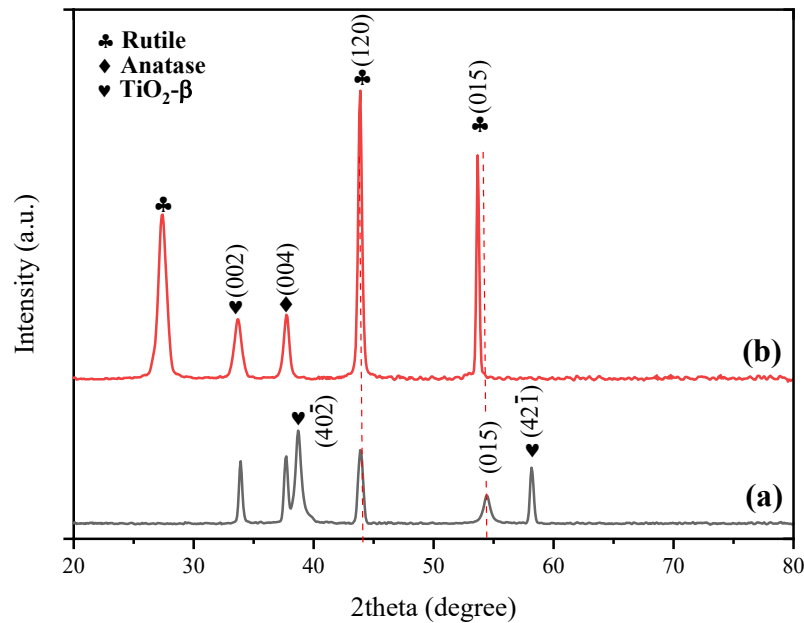
$$\left| \left( \frac{R_a - R_g}{R_g} \right) \right| \times 100\% \quad (2)$$

where  $R_a$  and  $R_g$  are the electrical resistance measured at the atmospheric air condition and the target gas atmosphere. The response ( $T_{res.}$ ) and recovery ( $T_{rec.}$ ) times were determined. The  $T_{res.}$  is the time required for the sensor resistance to reach 90% of its maximum change when exposed to the gas target (gas in), and  $T_{rec.}$  is the time required for the sensor resistance to returning to 10% of its initial value before exposure to the target gas (gas out) [19].

## Results and Discussion

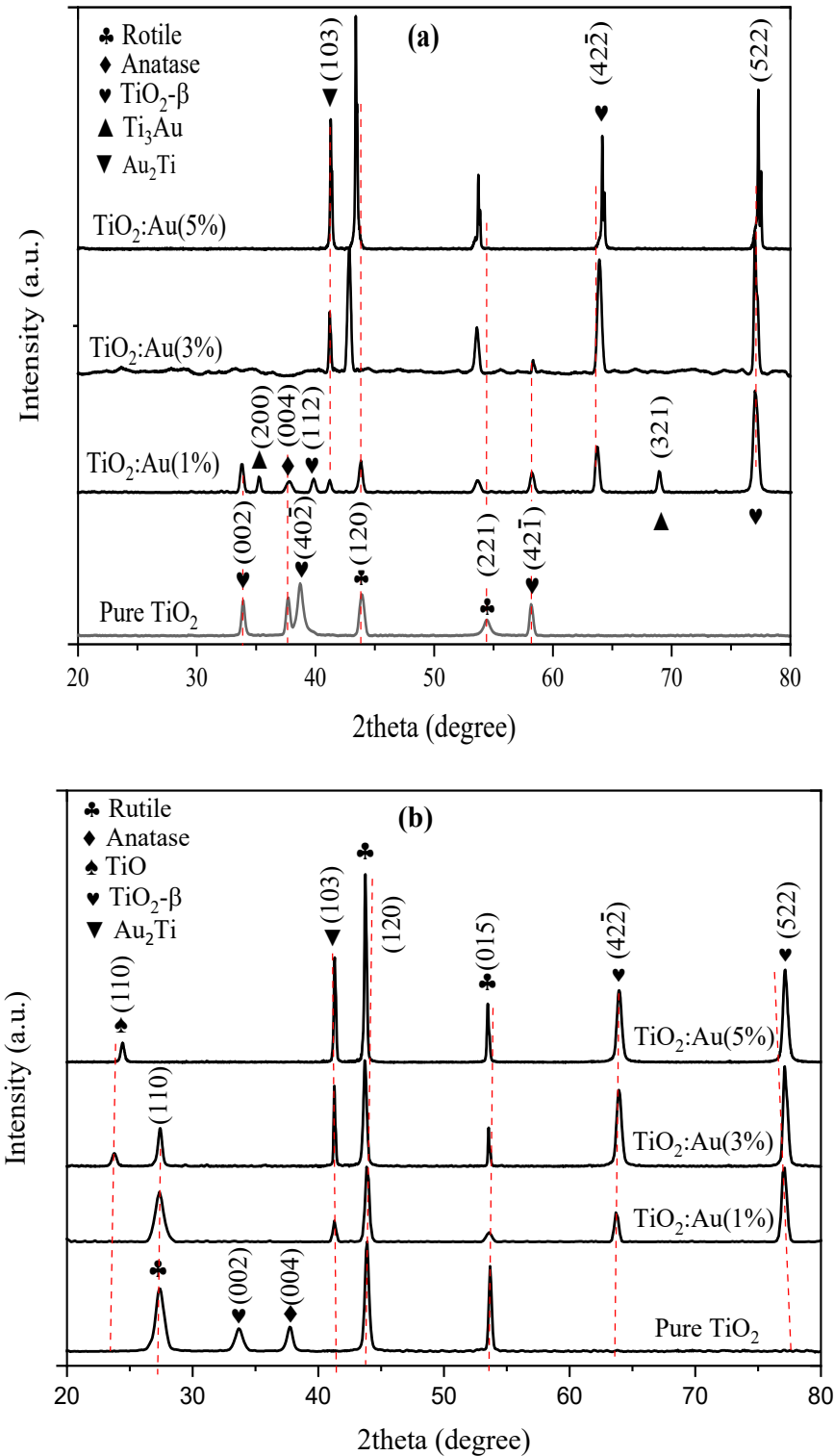
### Structural properties

Figure 2 shows the XRD pattern of the deposited  $TiO_2$  thin film on glass and Si (111) substrates. Figure 2a confirms the formation of a multi-phase structure of rutile, anatase, and  $\beta$ - $TiO_2$ , which corresponds to ICDS cards 00-021-1276, 98-000-9853, and 98-017-1670, respectively. Additionally, the rutile diffraction peak ( $40\bar{2}$ ) at  $2\theta$  around  $38.7^\circ$  was the dominating one, with a crystallite size of 54.2 nm, as illustrated in Figure 2a. The XRD pattern of  $TiO_2$  film deposited on a silicon substrate (Fig. 2b) revealed the formation of crystalline phases similar to those formed on the glass substrate, as well as the development of the rutile phase with a dominating crystalline orientation toward the diffraction peak (120) at  $2\theta = 27.3^\circ$  and crystallite size of 54.2 nm. When X-ray patterns of films deposited on silicon and glass substrates are compared, it becomes evident that the locations and intensities of the diffraction peaks differ, which could be attributed to variances in the substrate type and thermal stability of the  $TiO_2$  phases, which is consistent with the literature [20].



**Fig. 2: XRD patterns of TiO<sub>2</sub> and TiO<sub>2</sub> doped with Au thin films on (a) glass and (b) silicon substrates.**

The XRD patterns of TiO<sub>2</sub> thin films doped with various colloidal solution volume ratios of AuNPs deposited on glass and Si are shown in Figures 3a and 3b, respectively. At a volume of 1% AuNPs, the diffraction peak intensity decreased, and  $\beta$ -TiO<sub>2</sub> was the dominating phase structure toward the (522) diffraction peak with a crystallite size of 29 nm. At this vol% of silver nanoparticles, new mixed-phases of Ti<sub>3</sub>Au and Au<sub>2</sub>Ti were developed, matches respectively with the ICDD 00-007-032 and ICDD 00-029-065, referring to the Ti-Au bonding, as shown in figure 3a. When the AuNPs concentration increased to 3%, the crystallite size improved to 34.4 nm, and the intensity of the diffraction peaks increased significantly, indicating the stability of the same dominant phase and the absence of low-intensity diffraction peaks. The Au<sub>2</sub>Ti rutile phase was dominated with a preferred orientation toward (120) diffraction peak. The crystallite size was 53.2 nm when the vol% of AuNPs increased to 5%. Figure 3b illustrates the XRD pattern of TiO<sub>2</sub>: Au thin films deposited on Si substrate, and it shows the same growth behavior of those deposited on glass substrates. In terms of the domination phase, the  $\beta$ -TiO<sub>2</sub> phase was dominant at AuNPs solution volume of 1% and 3%, while the rutile phase was at 5%. In the same context, the  $\beta$ -TiO<sub>2</sub> phase was more growth with an increase of AuNPs vol%, and the rutile phase was dominant when the AuNPs vol% raised to 3% and 5%. Increasing the diffraction peaks intensity with the AuNPs volume concentration increases revealed that the gold nanoparticles contributed to the improved structural growth of the prepared films. The improvement in structural growth can be explained as follows: as the concentration of AuNPs rises, more bonds are formed, increasing the intensity of the characteristic peaks of deposited Ti-Au clusters on glass and silicon substrates [20].



**Fig. 3:** XRD patterns of undoped and Au doped  $\text{TiO}_2$  films on (a) glass and (b) silicon substrates.

### FE-SEM analysis

Fig. 3a-c shows the FE-SEM images of the  $\text{TiO}_2$ : Au thin films at various Au concentrations. These images demonstrate a heterogeneous distribution of different-sized grains, ascribed to the accumulation of  $\text{Ti}_3\text{Au}$  and  $\text{Au}_2\text{Ti}$  phases on the film surfaces. The sizes of the clusters were (54-180) nm, (31-162) nm, and (20-186) nm for 1, 3, and 5 at vol%, respectively. Some clusters showed concave character, especially for sample 5 at vol% Au, Fig. 3c. These structures may be formed due to the different surface energy of the  $\text{TiO}_2$  and Au-Ti composite, leading to the segregation of impurity phenomena where the small clusters are accumulated at the liquid phase. The Ti-Au diffraction peaks

confirm this behavior in Figures 2a and 2b, in good agreement with the theoretical modeling in the literature [9].

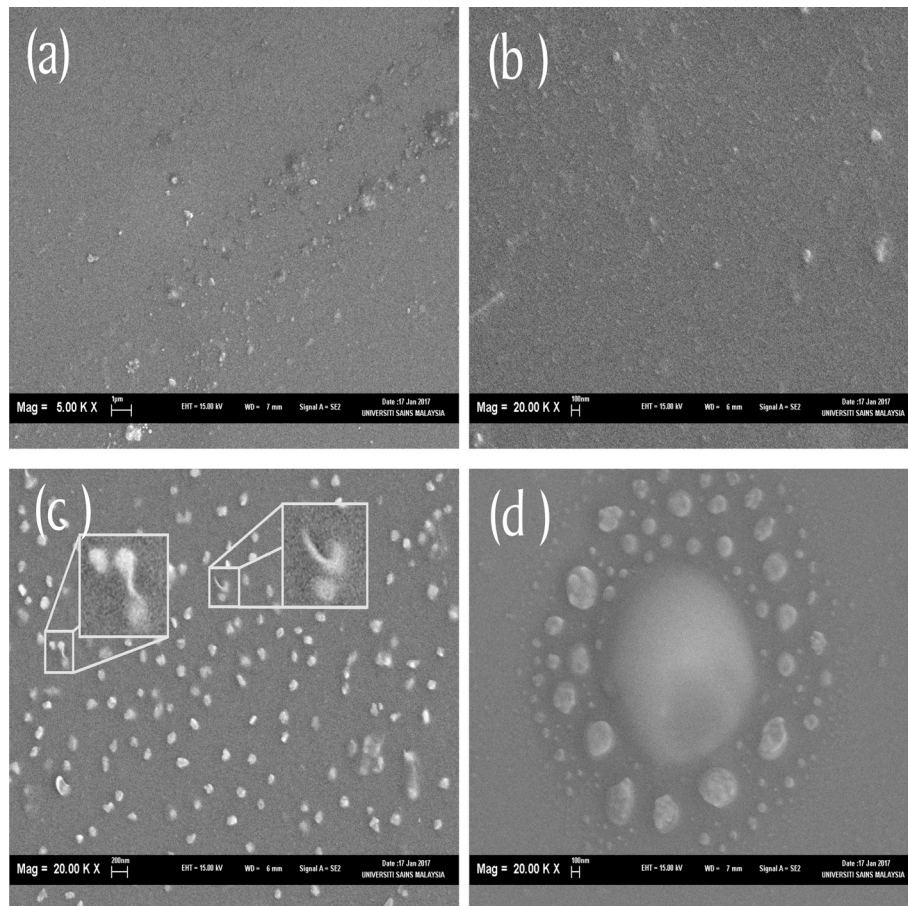


**Fig. 3:** FE-SEM images of  $\text{TiO}_2$ : Au thin films on Si substrates with Au at. vol% of (a) 1% (b) 3% (c) 5%, and (d) composition segregation of impurity for 5 at. vol% doped-sample.

### Gas sensor measurements

Figures 4 and 5 reveal the sensitivity% of the undoped and AuNPs-doped  $\text{TiO}_2$  thin films deposited on glass and silicon substrates at various operating temperatures when exposed to 30 ppm  $\text{H}_2\text{S}$ . As expected, the as-deposited  $\text{TiO}_2$  thin films on glass and silicon substrates exhibit low sensitivity improvement with increasing operating temperature, which can be attributed to the chemical inertness of the film surfaces at these operating temperatures. In contrast, the sensitivity of  $\text{TiO}_2$  films doped with AuNPs increased with increasing AuNPs concentration and operating temperature. Figures 4 and 5 show that the sample doped with 1% of gold nanoparticles deposited on glass substrate did not respond significantly below  $150^\circ\text{C}$  compared to the sample deposited on silicon substrates at the same doping ratio. The maximum sensitivity was obtained using a dopant ratio of 5% AuNPs for films formed on silicon and glass substrates, which were 121.20 % and 78.90 %, respectively, as shown in Table 1. The maximum sensitivity at 5% AuNPs can be attributed to the increase in the surface roughness as the concentration of AuNPs rises, as shown in Fig. 3c of the FE-SEM images. Also, increasing the temperature of n-type semiconductors, such as  $\text{TiO}_2$ , creates oxygen vacancies responsible for adsorbing sulfur atoms [6]. The fast response was 1.5 sec for the 1% AuNPs doped film on Si at  $200^\circ\text{C}$ , while the fast recovery time was 0.5 sec achieved by the 5% AuNPs doped sample on glass at  $200^\circ\text{C}$ .

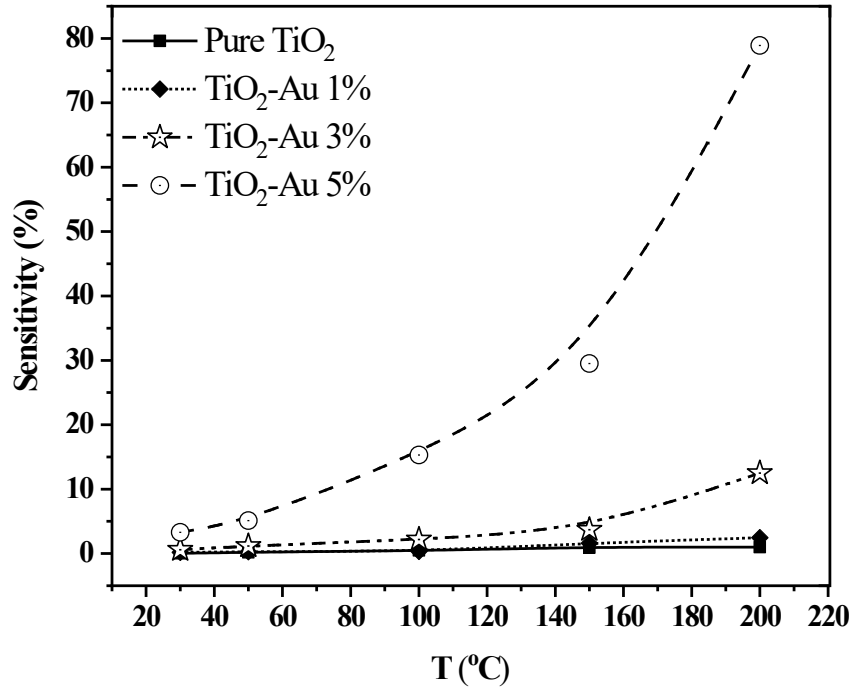


Fig. 4: Sensitivity of the tested films on glass substrates at different operating temperatures (T).

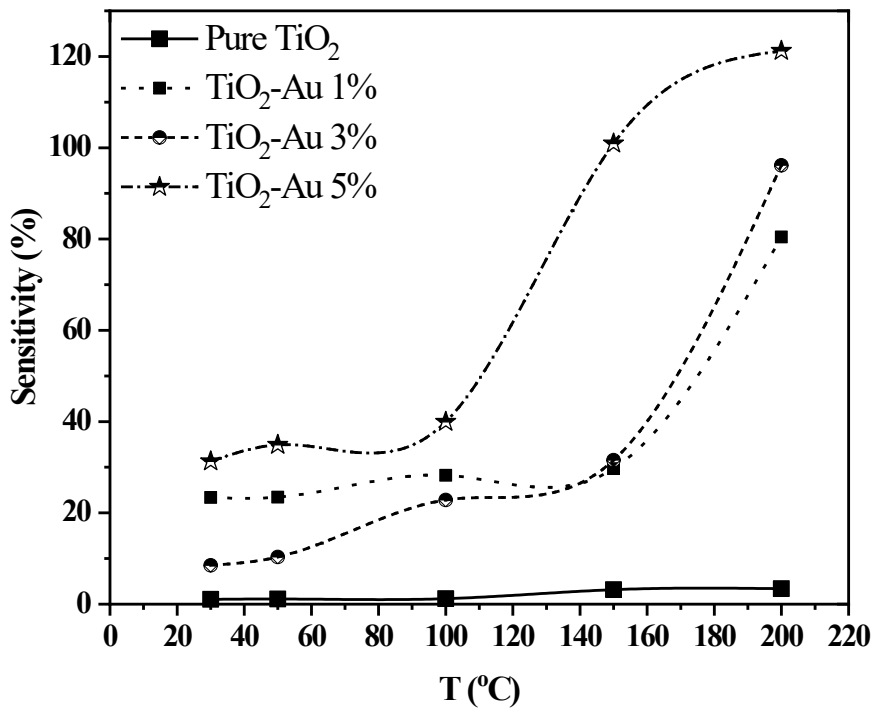
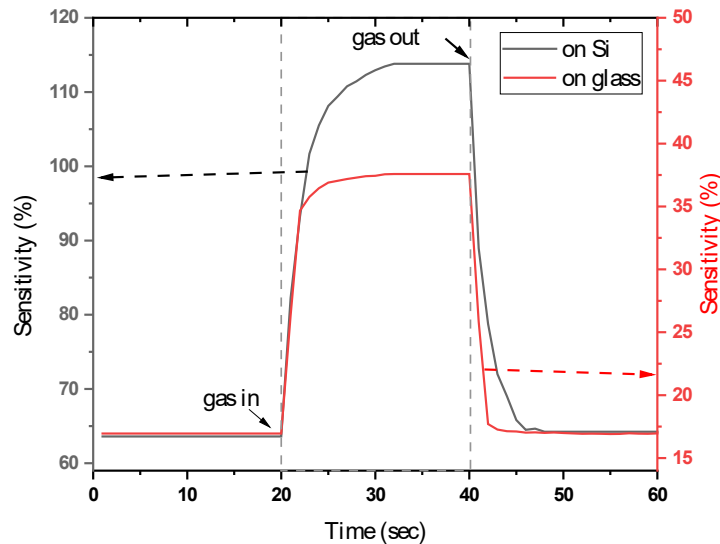


Fig. 5: Sensitivity of the tested films on silicon substrates at different operating temperatures (T).

**Table 1: The sensitivity, response, and recovery times of TiO<sub>2</sub> and TiO<sub>2</sub>: Au thin films.**

Parameter	T [°C]	On glass				On Silicon			
		TiO <sub>2</sub>	TiO <sub>2</sub> : Au (1%)	TiO <sub>2</sub> : Au (3%)	TiO <sub>2</sub> : Au (5%)	TiO <sub>2</sub>	TiO <sub>2</sub> : Au (1%)	TiO <sub>2</sub> : Au (3%)	TiO <sub>2</sub> : Au (5%)
Sensitivity (%)	RT	0.03	0.18	0.58	3.3	1.14	23.46	10.32	34.91
	50	0.18	0.29	1.18	5.1	1.21	28.22	22.83	39.96
	100	0.49	0.33	2.17	15.3	3.16	29.7	31.54	100.95
	150	0.91	1.61	3.69	29.5	3.15	29.70	31.50	100.90
	200	0.99	2.45	12.5	78.9	3.4	80.40	96.20	121.20
T <sub>Res.</sub> [sec]	RT	10.00	8.00	10.70	10.70	11.50	4.60	10.50	40
	50	10.10	5.91	12.60	9.20	9.87	6.10	6.10	6.10
	100	10.40	10.50	11.30	9.00	5.10	5.70	6.60	6.25
	150	4.80	13.50	10.40	9.60	10.50	2.30	7.60	5.60
	200	10.80	13.80	13.80	2.30	8.20	1.50	3.90	2.60
T <sub>Rec.</sub> [sec]	RT	9.20	9.20	6.60	11.60	6.80	6.10	13.20	6.60
	50	7.60	6.70	10.90	11.70	6.33	4.38	4.38	4.38
	100	12.20	5.30	14.40	11.70	2.91	5.10	3.40	2.92
	150	12.20	12.70	14.90	11.80	5.80	2.90	4.90	2.90
	200	4.70	13.30	13.30	0.50	3.50	3.20	2.20	1.70

The electrical resistance behavior of the sample with the highest response (5% AuNPs) was adopted to study the behavior of the sensor when exposed to H<sub>2</sub>S gas, as shown in Fig. 6. However, H<sub>2</sub>S gas adsorption on the TiO<sub>2</sub> sensor surface can affect its electrical conductivity when exposed to the gas target due to the interaction between TiO<sub>2</sub> and H<sub>2</sub>S [21]. Furthermore, at 5% AuNPs doping ratios, the more crystallization of the Au<sub>2</sub>Ti phase produces complex compounds due to the association of sulfite roots and AuNPs, which contributes to an increase in the rate of gas adsorption on the surface of TiO<sub>2</sub> films [9].

**Fig. 6: The sensitivity of the 5% AuNPs doped TiO<sub>2</sub> sample on (a) glass and (b) Si substrates at 200 °C.**



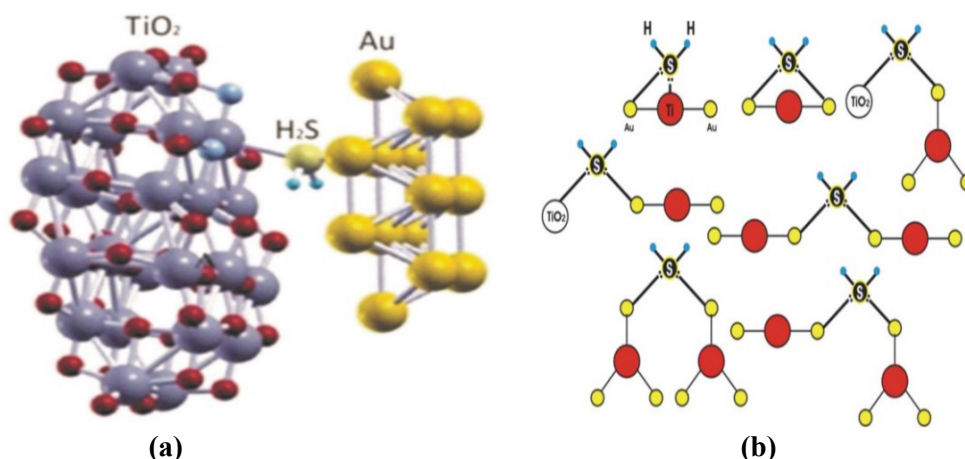


**Fig. 7: (a) Forming of Ti-S-Au linkages [9] and (b) the possible contacts of the sulfur atom with the surface composites during adsorption processes.**

The AuNPs supported chemical activity on the surface of TiO<sub>2</sub> that directly contributed to the formation of an island-like surface that added surface area for exposure of gas molecules on the surface of the sensor. The island-like structure distribution of the Au-Ti played a role in settlement gas molecules on the surface by forming Ti-S and Au-S bonds (Fig. 7a), increasing the electrical resistance of the film [22]. Ti-Au alloys are naturally like quantum dots [21], which have an abundance of electrons that make it simple to bond with sulfur atoms, resulting in electrical resistance change. Figure 7b depicts the potential interactions of the sulfur atom with surface composites during adsorption processes.

## Conclusion

The spray pyrolysis technique was successfully used to deposit TiO<sub>2</sub> and TiO<sub>2</sub>: Au thin films on glass and silicon substrates. XRD analysis of a coupled phase of TiO<sub>2</sub> and Ti-Au confirmed the existence of gold nanoparticles in the titanium dioxide structure. FE-SEM results revealed that the AuNPs varied the size of the surface-accumulated clusters between 20 and 186 nm. The TiO<sub>2</sub> and TiO<sub>2</sub>: AuNPs gas sensors on Si substrate displayed a higher sensitivity response than on a glass substrate when subjected to 30 ppm of H<sub>2</sub>S at the same operating temperatures. The dopant ratio of 5% AuNPs achieved the maximum sensitivity, confirming that the AuNPs support the chemical activity on the TiO<sub>2</sub> surface. The gas sensor samples also showed a fast response and recovery times, showing that the TiO<sub>2</sub>-Au NPs sensor devices are well-suited for H<sub>2</sub>S sensing applications. As a recommendation, the effect of crystalline phases formed by doping the semiconductors with metal nanoparticles on the sensitivity characteristics of gas sensors should be considered due to their significant contribution to improving these characteristics.

## References

- [1] S. Pawar, M. Chougule, S. Patil, B. Raut, D. Dalvi, P. Patil, S. Sen, P. Joshi, V. Patil, Fabrication of Nanocrystalline TiO<sub>2</sub> Thin Film Ammonia Vapor Sensor, *J. Sens. Technol.* 01 (01) (2011) 9–16.
- [2] J. Qiu, S. Zhang, H. Zhao, Recent applications of TiO<sub>2</sub> nanomaterials in chemical sensing in aqueous media, *Sensors Actuators B Chem.* 160 (1) (2011) 875–890.
- [3] S.S. Kaduory, A. Yousif, A.J. Haider, K.Z. Yahya, Annealing Effect on the Growth of Nanostructured TiO<sub>2</sub> Thin Films by Pulsed Laser Deposition (PLD), *Eng. T Ech. Jour Nal.* 31 (4) (2013) 460–470.
- [4] E. Cavaliere, G. Benetti, G.L. Celardo, D. Archetti, P. Pingue, G. Ferrini, L. Gavioli, Aggregation and fractal formation of Au and TiO<sub>2</sub> nanostructures obtained by fs-pulsed laser deposition: experiment and simulation, *J. Nanoparticle Res.* 19 (9) (2017) 311.

- 
- [5] H. Zhang, B. Chen, J.F. Banfield, G.A. Waychunas, Atomic structure of nanometer-sized amorphous TiO<sub>2</sub>, *Phys. Rev. B.* 78 (21) (2008) 214106.
- [6] C. Yanxin, J. Yi, L. Wenzhao, J. Rongchao, T. Shaozhen, H. Wenbin, Adsorption and interaction of H<sub>2</sub>S/SO<sub>2</sub> on TiO<sub>2</sub>, *Catal. Today.* 50 (1999) 39–47.
- [7] S. Park, S. Kim, S. Park, W. Lee, C. Lee, Effects of Functionalization of TiO<sub>2</sub> Nanotube Array Sensors with Pd Nanoparticles on Their Selectivity, *Sensors.* 14 (9) (2014) 15849–15860.
- [8] Y. Wang, T. Wu, Y. Zhou, C. Meng, W. Zhu, L. Liu, TiO<sub>2</sub>-Based Nanoheterostructures for Promoting Gas Sensitivity Performance: Designs, Developments, and Prospects, *Sensors.* 17 (9) (2017) 1971.
- [9] A. Abbasi, J. Jahanbin Sardroodi, Adsorption of H<sub>2</sub>S molecule on TiO<sub>2</sub>/Au nanocomposites: A density functional theory study, *Nanochemistry Res.* 2 (1) (2017) 1–7.
- [10] K.M. Garadkar, B.S. Shirke, P.P. Hankare, D.R. Patil, Low Cost Nanostructured Anatase TiO<sub>2</sub> as a H<sub>2</sub>S Gas Sensor Synthesized by Microwave Assisted Technique, *Sens. Lett.* 9 (2) (2011) 526–532.
- [11] G.N. Chaudhari, D.R. Bambole, A.B. Bodade, P.R. Padole, Characterization of nanosized TiO<sub>2</sub> based H<sub>2</sub>S gas sensor, *J. Mater. Sci.* 41 (15) (2006) 4860–4864.
- [12] W.P. Jakubik, Investigations of Thin Film of Titanium Dioxide ( TiO<sub>2</sub> )in a Surface Acoustic Wave Gas Sensor System, *Mol. Quantum Acoust.* 27 (2006) 133–139.
- [13] E. Della Gaspera, M. Guglielmi, S. Agnoli, G. Granozzi, M.L. Post, V. Bello, G. Mattei, A. Martucci, Au Nanoparticles in Nanocrystalline TiO<sub>2</sub> –NiO Films for SPR-Based, Selective H<sub>2</sub>S Gas Sensing, *Chem. Mater.* 22 (11) (2010) 3407–3417.
- [14] E. Gazzola, M. Cittadini, M. Angiola, L. Brigo, M. Guglielmi, F. Romanato, A. Martucci, Nanocrystalline TiO<sub>2</sub> Sensitive Layer for Plasmonic Hydrogen Sensing, *Nanomaterials.* 10 (8) (2020) 1490.
- [15] L. FRANCIOSO, A. TAURINO, A. FORLEO, P. SICILIANO, TiO<sub>2</sub> nanowires array fabrication and gas sensing properties, *Sensors Actuators B Chem.* 130 (1) (2008) 70–76.
- [16] M.A. Al-Alousi, I.M. Ibrahim, N.I. Fawz, Effect of laser energy and pulses on size and concentration of gold nanoparticles in DDDW by LALP method, *Iraqi J. Phys.* 14 (30) (2019) 112–119.
- [17] P. Perillo, D. Rodríguez, TiO<sub>2</sub> Nanotubes Membrane Flexible Sensor for Low-Temperature H<sub>2</sub>S Detection, *Chemosensors.* 4 (3) (2016) 15.
- [18] B.E. Al-Jumaili, J.M. Rzaïj, A.S. Ibraheam, Nanoparticles of CuO thin films for room temperature NO<sub>2</sub> gas detection: Annealing time effect, *Mater. Today Proc.* 42(2021) 2603-2608.
- [19] J.M. Rzaïj, Characterization of CuO thin films for gas sensing applications, *Iraqi J. Phys.* 14 (31) (2019) 1–12.
- [20] C.P. Lin, H. Chen, A. Nakaruk, P. Koshy, C.C. Sorrell, Effect of Annealing Temperature on the Photocatalytic Activity of TiO<sub>2</sub> Thin Films, *Energy Procedia.* 34 (2013) 627–636.
- [21] S. Mubeen, T. Zhang, N. Chartuprayoon, Y. Rheem, A. Mulchandani, N. V Myung, M.A. Deshusses, Sensitive Detection of H<sub>2</sub>S Using Gold Nanoparticle Decorated Single-Walled Carbon Nanotubes, *Anal. Chem.* 82 (1) (2010) 250–257.
- [22] G. Zheng, L. Xu, Y. Zhan, Y. Wu, C. Zhang, Gold Nanoparticle Embedded Titanium Dioxide Thin Film for Surface Plasmon Resonance Gas Sensing at Room Temperature, *Sens. Lett.* 11 (11) (2013) 2038–2042.